*29th EPS Conference on Plasma Phys. and Contr. Fusion Montreux, 17-21 June 2002 ECA Vol. **26B**, P-2.044 (2002)*

Real-time control of the current profile in JET

D. Mazon[1], X. Litaudon[1], D. Moreau[1], A. Bécoulet[1], J.M.Chareau[1], F.Crisanti[2], R. Felton[3], E. Joffrin[1], M. Mantsinen[4], A. Murari[5], V.Pericoli-Ridolfini[2], M. Riva[2], G. Tresset[1], L. Zabeo[1], K.D. Zastrow[3] and contributors to the EFDA-JET workprogramme.

[1]*Association Euratom-CEA, CEA Cadarache, F-13108, St Paul lez Durance, France*
[2]*Associazione Euratom-ENEA sulla Fusione, C.R. Frascati, 00044 Frascati, Italy*
[3]*EURATOM/UKAEA Fusion Association, Culham Science Centre, Abingdon, U. K.*
[4]*Association Euratom-Tekes, Espoo, Finland*
[5]*Consorzio RFX Associazione ENEA-EURATOM per la Fusione, 4-35127 Padova, Italy*

1) Introduction

The transport reduction observed in a number of tokamak devices has been associated with localised turbulence suppression, which is related with both plasma magnetic shear and flow shearing rate. Moreover, the strong correlation between the triggering of an internal transport barrier (ITB) and the appearance of integer-q-magnetic surfaces at particular locations has also been shown [1]. New real-time systems and control algorithms have therefore been developed and implemented in JET for controlling the ITB dynamics and the current density profile. Confinement parameters [2], electron temperature [3], particle and current density profiles [4] are now available in real-time using magnetic, electron cyclotron emission and interfero-polarimeter data, thus allowing kinetic and magnetic profile control.

2) Current profile identification algorithm

The successful results of the last JET experimental campaign [5], related to the real-time control of ITBs in high performance plasmas with a large bootstrap fraction through local quantities characteristic of the ITB strength [6] have shown that active control of the current density profile was very beneficial to the sustainment of the barrier in steady state.

Up to now, control of the q-profile was performed through feedback control of the internal inductance parameter, l_i [7]. An example of such a control using lower hybrid current drive (LHCD) as actuator during a preheat phase in JET is shown in Fig.1. However l_i is a global quantity characterizing mainly the current density in the outer plasma layers and its control is not sufficient to maintain an optimum magnetic shear profile in ITB discharges. We have thus tried for the first time a direct control of the safety factor profile, and in the last section of this paper, a first "proof of principle" experiment will be reported.

Efforts have therefore been made in order to develop an algorithm which provides a measurement of the q-profile in real-time [4] and allows feedback control. The algorithm uses as inputs the signals of the magnetic and of the interferometer polarimeter diagnostics. The topology of the last closed magnetic surface (LCMS) is determined on the basis of the external magnetic pick-up coils measurements. To complete the magnetic topology in the interior of the plasma, the following flux surface parameterisation is used [8]:

$$\begin{cases} R = R_{axis} + \Delta(\rho) + \rho\cos(\vartheta + \gamma(\rho)\sin\vartheta) \\ Z = Z_{axis} + \rho K(\rho)\sin\vartheta \end{cases}$$

Where ρ is the radial co-ordinate, R_{axis} and Z_{axis} the co-ordinates of the magnetic axis, $\Delta(\rho)$ the Shafranov shift ($\Delta<0$), $\gamma(\rho)$ the triangularity and $K(\rho)$ expresses the elongation. A systematic analysis of the result of the equilibrium reconstruction code EFIT has shown that the radial dependences of the plasma shift, elongation and triangularity can be expressed satisfactorily by the following monotonic relations:

$$\Delta(\rho) = \left(\frac{\rho}{\rho_{LCMS}}\right)^{\alpha}\Delta_{LCMS}\,;\, K(\rho) = K_{axis} + a_2\left(\frac{\rho}{\rho_{LCMS}}\right)^{2} + a_4\left(\frac{\rho}{\rho_{LCMS}}\right)^{4}\,;\, \gamma(\rho) = \gamma_{LCMS}\left(\frac{\rho}{\rho_{LCMS}}\right)^{\beta}$$

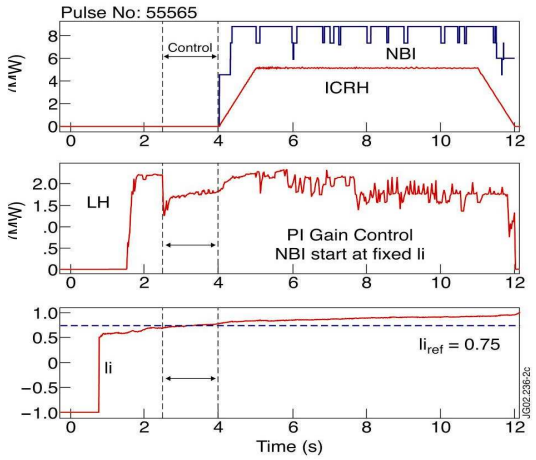

Fig.1 : Real-time control of the internal inductance during the preheat phase with LHCD as actuator (#55565, B_T=3.4T,Ip=1.8MA).Control starts at 42.5s

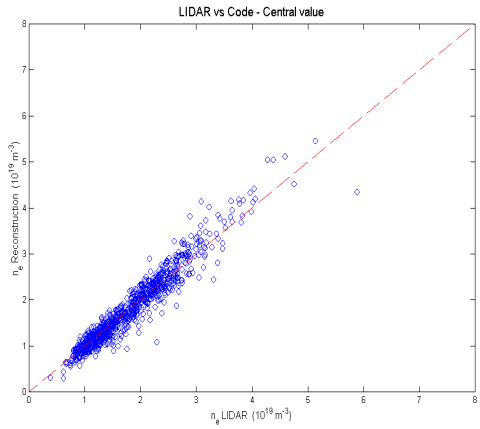

Fig.2: Comparison of LIDAR central density value with the one obtained by the inversion technique.

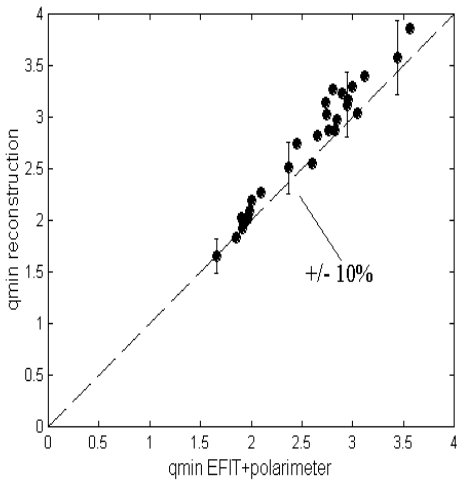

Fig.3: Comparison between the minimum of the real-time safety factor and the one obtained from EFIT+polarimetry.

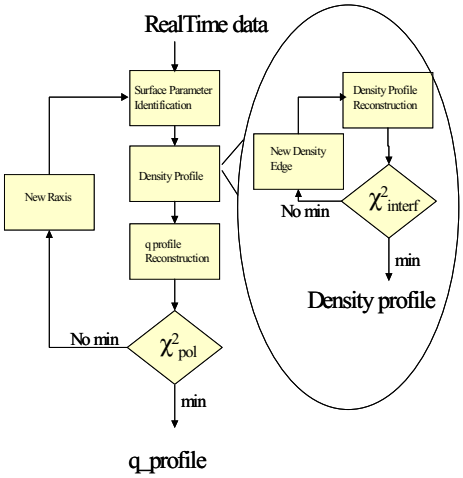

Fig.4 : Block diagram of the algorithms for the reconstruction of the density and *q* profiles.

The constants in the previous equations are determined from the component of the poloidal field at the edge, measured by the pick up coils.

$$B_p^R(\rho,\vartheta) = -\frac{1}{2\pi R}\frac{\partial \Psi}{\partial \rho}\frac{\partial \rho}{\partial Z} \qquad B_p^Z(\rho,\vartheta) = \frac{1}{2\pi R}\frac{\partial \Psi}{\partial \rho}\frac{\partial \rho}{\partial R}$$

where Ψ is the poloidal flux. Once the magnetic surface geometry has been determined, the line integrated measurements of the interferometer are inverted with SVD techniques using the following parameterisation for the density:

$$n_e(\rho) = n_0(1-\rho^2)(1+p\rho^2+q\rho^4)+n_w$$

This provides n_0, n_0p, n_0q, the pedestal value n_w being scanned in order to minimize in the least square sense the square difference between the experimental measurements and the calculated one. The method is similar for the determination of the poloidal field through the polarimetric data which is taken along the same line of sight of the interferometer. The inversion procedure of these integral measurements provides the poloidal field value in each points of the determined magnetic surfaces and therefore allows the calculation of the safety factor profile q at the same points, since the toroidal field is known. Comparison in Fig.2 between the central density obtained from the previous algorithm and LIDAR shows a fair agreement. The same conclusion is reached for the minimum safety factor q_{min} obtained in real-time compared to EFIT constrained with polarimetry data Fig.3. A summarize of the q-

profile algorithm reconstruction is depicted in Fig.4. One of the multiple interests of the availability of the q-profile in real-time is for example the triggering of the main heating phase on a particular value of q_{min}, which has been identified as a main component in the ITB formation. An example is given in Fig.5 where ion cyclotron resonant heating (ICRH) and neutral beam injection (NBI) are triggered at a time when $q_{min}= 3$.

3) Model-based profile control technique

Due to the strong non-linear couplings between pressure and current density profiles and the multiple time scales involved in the transport processes, advanced feedback schemes have to be developed to control high-β, high-bootstrap-fraction, ITB discharges and maintain the plasma in steady state, away from MHD limits. Schemes for tailoring the current profile in ITER-FDR advanced scenarii have been examined earlier [9] pointing out the main issues of the problem. They were based on decoupled loops controlling q(r) and Ψ(r) at two radii with devoted actuators. A new approach (cf. [10] for details) is followed here, in which more information on the spatial structure of the system is taken into account by retaining its distributed nature, and considering the non-local interaction between various quantities through a diffusion-like operator. A linearized Laplace transform model of the form $\mathbf{Q}(s) = \mathbf{K}(s)\ \mathbf{P}(s)$, where **Q** represents a safety factor difference vector and **P** an input power difference vector, is assumed around the target plasma steady state. The kernel **K**(s) can be identified from power modulation experiments around the target steady state, or by simulating such experiments using a predictive transport code. For the experiments described below, however, the steady state gain matrix **K**(0) was sufficient and was deduced from simple step power changes in dedicated open loop experiments. Then a truncated singular value decomposition is performed yielding $\mathbf{K}(0) = \mathbf{W}\,\mathbf{\Sigma}\,\mathbf{V}^+$ with $\mathbf{V}^+$ the transpose matrix of **V** and this provides steady state decoupling between modal inputs $\boldsymbol{\alpha}(s) = \mathbf{V}^+\ \mathbf{P(s)}$, and modal outputs $\boldsymbol{\beta}(s) = \mathbf{W}^+\ \mathbf{Q}(s)$, namely $\boldsymbol{\beta}(0) = \mathbf{\Sigma}\ \boldsymbol{\alpha}(0)$. Pseudo-modal control techniques can therefore be used by inverting the diagonal steady state gain matrix, **Σ**. In order to obtain a simple proportional-plus-integral feedback control with minimum (least square) steady state offset, we chose the controller transfer function matrix **G**(s) as follows

$$\boldsymbol{\alpha}(s) = \mathbf{G}(s)\ .\ \boldsymbol{\beta}(s) = g_c\,[1 + 1/(\tau_i.s)]\ \mathbf{\Sigma}^{-1}\ \boldsymbol{\beta}(s)$$

where g_c is the proportional gain and (g_c/τ_i) is the integral gain.

4) Experimental results

A direct application of the control scheme described above was to reach a predefined q-profile target in conditions where all other plasma parameters are maintained constant. The experiment was thus performed during an extended LHCD preheat phase and could be followed in a long-pulse machine by the application of the main neutral beam heating power for ITB triggering once the desired optimised q-profile target has been obtained. The central line-integrated density was maintained constant at $2.7 10^{19} m^{-2}$ during the whole pulse, a relatively low density which allows efficient LHCD. The toroidal field was 3T and in order to be close to a non-inductive steady state regime and thus have a larger flexibility for obtaining non-ohmic reduced-shear q-profiles, the plasma current was fixed at 1.5MA. The feedback control was performed on five points of the q-profile located at fixed normalised radii (r/a=0.2,0.4,0.5,0.6,0.8). The global result is shown in Figure 6. We can see that the target q-profile (red curve) is reached, the controller minimizing in the least square sense the difference between the target q-values and the real-time measurements. In fig.7 the time traces of the 5 measured and required q-values and the LHCD power waveform are presented. A comparison with a pulse in similar experimental conditions but with no feedback control shows the efficiency of the control in preventing the monotonic relaxation of the q-profile towards a peaked ohmic profile.

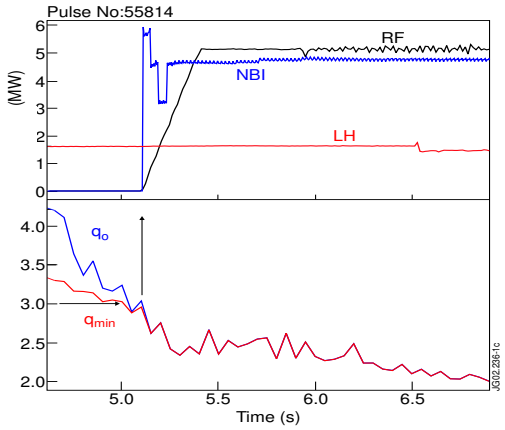

Fig.5 : Triggering of main heating power at a rational q_{min} value (q_{min}=3). (#55814, B_T=3.4T,Ip=1.8MA).

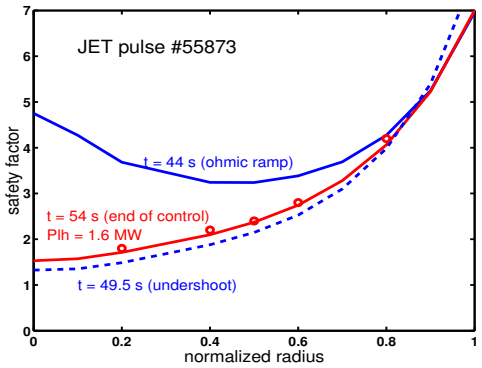

Fig.6 : Real-time control of the q-profile (5 values at 5 radii) using model based control with LHCD as actuator (#55873, B_T=3T, Ip=1.5MA).

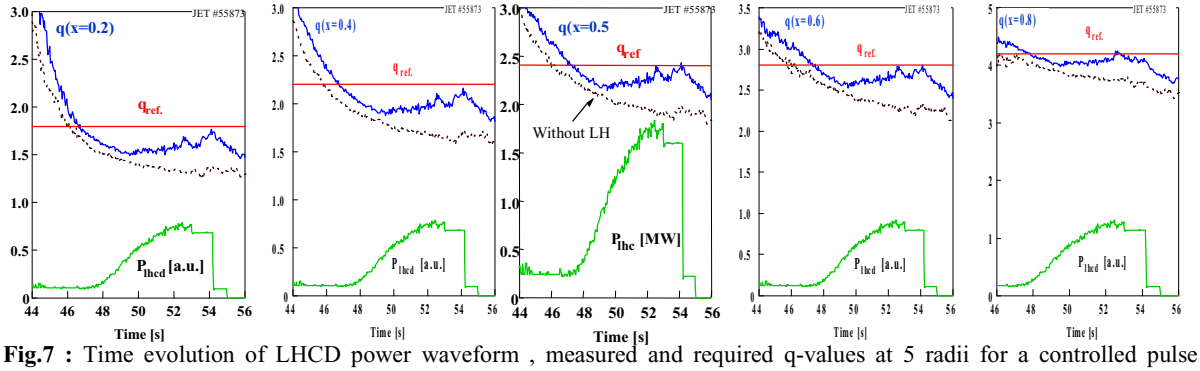

Fig.7 : Time evolution of LHCD power waveform , measured and required q-values at 5 radii for a controlled pulse (#55873 B_T=3T, Ip=1.5MA). A pulse (#55871 B_T=3T,Ip=1.5MA) without feedback control is presented for comparison. Control starts at 42s and stops at 53.5s.

5) Conclusion

The current density profile is now available in real-time at JET and has been extensively validated during the last campaign. A first successful demonstration has been made concerning the feedback control of the safety factor during a low density phase using LHCD as the only actuator. A further objective in future experimental campaigns will be to control the q-profile during the main heating phase in the presence of an ITB at higher density and therefore with a large bootstrap current component. Then, using the combined heating and current drive systems, the model-based algorithm described above will be applied to the simultaneous control of both pressure and current profiles in the aim of extending the duration of high performance ITB plasmas towards steady state operation.

References

[1] E. Joffrin, et al 2002 Plasma. Phys. Control. Fusion, **44,** to appear.
[2] O.Barana et al 2002 Rev. of Scient. Instrum, submitted for publication.
[3] M. Riva et al 2002 Proc. 19th IEEE/NPSS Symp on Fusion Eng. (SOFE) (Atlantic City, USA January 2002).
[4] L.Zabeo et al 2002 Plasma. Phys. Control. Fusion, to appear.
[5] D.Mazon et al 2002 Plasma. Phys. Control. Fusion, **44,** to appear.
[6] G. Tresset et al 2002 Nucl. Fusion **42**, 520.
[7] T. Wijnands et al 1997 Nucl. Fusion **37**, 777.
[8] J.P Christiansen et al 1987 Journal of computational Physics **73**, 85.
[9] D.Moreau, I. Voitsekhovitch, 1999, Nucl. Fusion **39**, 685.
[10] D.Moreau et al, Proc. of the 3nd IAEA TCM on Steady State Operation of Magnetic Fusion Devices, May 2002 ; to be published in Nucl. Fusion.